



Erosion potential of ultrasonic food processing

Sergei A. Bredihin¹, Vladimir N. Andreev¹, Alexander N. Martekha^{1,*},
Matthias G. Schenzle², Igor A. Korotkiy³

¹ K.A. Timiryazev Russian State Agrarian University^{ROR}, Moscow, Russia

² VA GmbH Society for Food Processing, Stuttgart, Germany

³ Kemerovo State University^{ROR}, Kemerovo, Russia

* e-mail: man6630@rgau-msha.ru

Received April 30, 2021; Accepted in revised form May 21, 2021; Published online October 15, 2021

Abstract:

Introduction. Cavitation is the most significant factor that affects liquid food products during ultrasound treatment. Ultrasonic treatment intensifies diffusion, dissolution, and chemical interactions. However, no physical model has yet been developed to unambiguously define the interaction between ultrasonic cavities and structural particles of liquid food media. Physical models used to describe ultrasonic interactions in liquid food media are diverse and, sometimes, contradictory. The research objective was to study ultrasonic devices in order to improve their operating modes and increase reliability.

Study objects and methods. The present research featured ultrasonic field generated in water by the cylindrical emitter, the intensity of flexural ultrasonic waves and their damping rate at various distances from the emitter.

Results and discussion. The paper offers a review of available publications on the theory of acoustic cavitation in various media. The experimental studies featured the distribution of cavities in the ultrasound field of rod vibrating systems in water. The research revealed the erosion capacity of ultrasonic waves generated by the cylindrical emitter. The article also contains a theoretical analysis of the cavitation damage to aluminum foil in water and the erosive effect of cavitation on highly rigid materials of ultrasonic vibration systems. The obtained results were illustrated by semi-graphical dependences.

Conclusion. The present research made it possible to assess the energy capabilities of cavities generated by ultrasonic field at different distances from the ultrasonic emitter. The size of the contact spot and the penetration depth can serve as a criterion for the erosion of the surface of the ultrasonic emitter.

Keywords: Ultrasound, cavitation, aqueous medium, foil screen, erosion, oscillatory system

Funding: The research was carried out on the premises of the K.A. Timiryazev Russian State Agrarian University (RT SAU)^{ROR}, with financial support from the Ministry of Science and Higher Education of the Russian Federation (Minobrnauka)^{ROR} as part of the program for the development of world-class research center “Agrotechnology of the Future” (The grant was delivered as subsidies from the federal budget for state support of world-class research centers, performing R&D in scientific and technological priority areas, No. 075-15-2020-905 (internal number 00600/2020/80682), November 16, 2020).

Please cite this article in press as: Bredihin SA, Andreev VN, Martekha AN, Schenzle MG, Korotkiy IA. Erosion potential of ultrasonic food processing. *Foods and Raw Materials*. 2021;9(2):335–344. <https://doi.org/10.21603/2308-4057-2021-2-335-344>.

INTRODUCTION

Ultrasound technologies in the food and processing industries have been the focus of numerous studies. As a result, information about ultrasound treatment of food media is quite abundant. Cavitation is the main process of ultrasound treatment of liquids. Ultrasonic waves accelerate diffusion, chemical reactions, and dissolution processes in liquid foods. The ultrasonic acceleration of chemical interactions results from free ions formed during ultrasonic cavitation.

Contemporary food science knows no universally accepted theory that would unambiguously describe the physical nature of the interaction of ultrasonic cavities and structural particles during food processing. The existing physical models are diverse and often contradictory. They give a very vague explanation of the processes that occur in the ultrasonic field. According to some models, cavities have high pressures and temperatures. According to others, cavitation creates microcavities of deep vacuum and cryogenic temperatures. Both destroy microparticles in liquid

media. For instance, ultrasonic cavities break milk fat globules into smaller fragments [1–5]. Cavitation is the formation of microcavities in a liquid medium, which are called bubbles, voids, or just cavities. These cavities are filled with vapor phase, gas, or a mixture of both. Cavities are formed in local zones of the liquid phase, where the pressure drops to a critical level, which usually coincides with the saturation pressure. Hydrodynamic cavities develop in a flow of fluid; acoustic cavities develop as a result of acoustic treatment [3].

Physical models of cavitation can be contradictory because experimental studies of cavitation are quite complex. To be used in food industry, ultrasonic cavitation requires optimal operating modes of ultrasonic devices. Reliability and safety of ultrasonic devices remain an important issue of food science [6–8].

Cavitation theories. The ability of ultrasound to accelerate food processing was established in the early XX century. For example, such phenomena as the acceleration of water-fat emulsion or finely dispersed suspensions are quite old. In 1960s, ultrasonic treatment began to be used in chocolate production: it provided a more effective mixing, emulsification, and better dispersion. However, these methods found little practical use because of their economic inexpediency. Ultrasound methods and technical means used to be imperfect and expensive [9, 10].

The latest technology of controlled, focused, and highly intensive ultrasonic field had low energy costs, which made it economically feasible. As the technology gained more popularity, it revealed some new opportunities. For example, ultrasound treatment raised the intensity of extraction in cognac production by hundreds of times. Similar beneficial effects were observed in other processes, e.g. extraction of vegetable oils.

However, high-intensity ultrasound technologies erode the device surfaces that come in direct contact with the product. As a result, the processed product might contain some components that are not part of the formulation. Studies of the interaction between the product and the surface of the ultrasonic cavitator (oscillatory system) can help reduce or eliminate erosion [11].

To find out more about various theories of collapse and waves of a single cavity, see [3–5]. The results of these researches made theoretical studies as reliable as actual practical experiments in cavitation.

In its most general form, the equation of motion of the outer wall of the cavity in spherical coordinates looks like this:

$$\frac{\partial u}{\partial t} + u \frac{\partial u}{\partial r} = -\frac{1}{\rho} \frac{\partial p}{\partial r} \quad (1)$$

where t – time, s; r – current radius, m; ρ – liquid density, kg/m³; p – hydrostatic pressure, Pa.

The continuity equation has the following form:

$$\frac{\partial}{\partial r}(r^2 u) = 0 \quad (2)$$

The vortex-free motion of the surface can be considered as a potential with potential φ , i.e.:

$$u = -\frac{\partial \varphi}{\partial r} \quad (3)$$

Provided the bubble surface is $r = R$, $u = U$, then:

$$u = U \left(\frac{R}{r} \right)^2 \quad (4)$$

Equations (3) and (4) produce the following result:

$$\varphi = U \frac{R^2}{r} \quad (5)$$

Integration of (1) from r to $r = \infty$ results in:

$$u - \frac{u^2}{2} + \int_{p_\infty}^{p(r)} \frac{dp}{\rho} = 0 \quad (6)$$

The condition of incompressibility of liquid means that $\rho = \rho_0 = \text{const}$; therefore, (6) is:

$$u - \frac{u^2}{2} + \frac{1}{\rho_0} [P_\infty - p(r)] = 0 \quad (7)$$

Inserting (5) in (7) at $r = R$, we get the following equation for an empty cavity:

$$\frac{1}{r} \left(\frac{R^2}{2} \frac{dU^2}{dR} + 2RU^2 \right) - \frac{1}{2} U^2 \frac{R^4}{r^4} + \frac{1}{\rho_0} [P_\infty - p(r)] = 0 \quad (8)$$

For cavity surface $r = R$, $U = dR/dt$; thus, equation (8) looks like this:

$$R \frac{d^2 R}{dt^2} + \frac{3}{2} \left(\frac{dR}{dt} \right)^2 + \frac{1}{\rho_0} [P_\infty - P(R)] \quad (9)$$

where $P(R)$ is cavity surface pressure.

The resulting equation describes the motion of the cavity surface depending on the regularity of the pressure change $P(R)$.

Lamb and Rayleigh obtained a solution to equation (9) assuming the simplest boundary conditions: $P(R) = 0$, $P_\infty = P_0$, i.e. pressure at a sufficient distance equals hydrostatic pressure:

$$U^2 = \frac{2}{3} \frac{P_0}{\rho_0} \left(\frac{R_m^3}{R^3} - 1 \right) \quad (10)$$

where R_m is maximal cavity radius early during collapse.

Provided $U = dR/dt$, we get Rayleigh's equation:

$$\tau = 0.915 R_m \left(\frac{\rho_0}{P_0} \right)^{1/2} \quad (11)$$

where τ is time of cavity collapse, s.

In the middle of the XX century, Nolting and Nepiras obtained an equation for cavity pulsations based on the Laplace surface tension forces and the change in the gas volume in the cavity during adiabatic expansion and compression [5]. They used harmonic pressure fluctuations as a boundary condition at a sufficient distance from the cavity. The equation is:

$$R \frac{d^2 R}{dt^2} + \frac{3}{2} \left(\frac{dR}{dt} \right)^2 + \frac{1}{\rho_0} \left[P_0 - P_s - P_m \sin(\omega t) + \frac{2\sigma}{R} - \left(P_0 + \frac{2\sigma}{R_0} \right) \left(\frac{R_0}{R} \right)^{3\gamma} \right] = 0 \quad (12)$$

where P_s – steam pressure in the cavity;

$\omega = 2\pi f$, f – oscillation frequency; σ – Laplace surface tension; γ – adiabatic exponent (4/3), ρ_0 – density of liquid unaffected by fluctuations, P_m – maximal pressure in the cavity attained at its minimal radius.

The numerical solutions proposed in [6, 7] describe the changes in the radius of the cavity. The speed of movement of the cavity surface approaches the speed of sound in a liquid medium. It is the boundary condition for the application of the abovementioned equations. The continuity equation under these conditions has the following form:

$$\frac{\partial \rho}{\partial t} + \frac{1}{r^2} \frac{\partial}{\partial r} (r^2 \rho u) = 0 \quad (13)$$

$$R \left(1 - 2 \frac{U}{c_0} \right) \frac{d^2 R}{dt^2} + \frac{3}{2} \left(1 - \frac{4U}{3c_0} \right) \left(\frac{dR}{dt} \right)^2 + \frac{1}{\rho_0} \left[P_0 - P_n - P_m \sin(\omega t) + \frac{2\sigma}{R} + \frac{4\eta U}{R} - \left(P_0 + \frac{2\sigma}{R_0} \right) \left(\frac{R_0}{R} \right)^{3\gamma} \right] + \frac{R U}{\rho_0 c_0} \left(1 - \frac{U}{c_0} \right) \frac{dP(R)}{dR} = 0 \quad (15)$$

Kirkwood and Bethe introduced the concept of specific enthalpy h and kinetic enthalpy:

$$\Omega = \frac{\partial \varphi}{\partial t} = h + \frac{u^2}{2} \quad (16)$$

Thus, they obtained an equation that describes cavity pulsations and takes into account the compression and surface tension of the liquid, as well as the polytropic (adiabatic) character of vapor expansion in the cavity:

$$R \left(1 - \frac{U}{c} \right) \frac{d^2 R}{dt^2} + \frac{3}{2} \left(1 - \frac{1U}{3c} \right) \left(\frac{dR}{dt} \right)^2 - \left(1 - \frac{U}{c} \right) H - \frac{U}{c} \left(1 - \frac{U}{c} \right) R \frac{dH}{dR} = 0, \quad (17)$$

where $c^2 = c_0^2 \left(\frac{\rho}{\rho_0} \right)^{n-1}$; $H = \int_{\rho_0}^{\rho} \frac{dp}{\rho} = \frac{c_0^2}{n-1} \left[\left(\frac{\rho}{\rho_0} \right)^{n-1} - 1 \right]$;

$$c = \left[c_0^2 + (n-1)H \right]; c_0^2 = An / \rho_0$$

where H – free enthalpy on the sphere surface; A and n – constants for water ($A = 3.001 \times 10^8 \text{ Pa} = 3.001 \times 10^5 \text{ MPa}$; $n = 7$).

An analysis of the equations of Nolting-Nepiras, Herring-Flynn, and Kirkwood-Bethe showed the similarity of the results, which diverged only at high ultrasound frequencies and in the case of a long collapse time [6].

The theory of shock waves during cavitation.

Many researchers performed visual observations and proved that the erosion of the surfaces within the cavitation field occurs due to the high local pressures that take up the form of shock waves when cavities collapse [12, 13].

The analysis of the propagation of spherical shock waves consists in determining function $G(R, t)$ on the cavity surface with radius R and calculating the time it takes the waves to appear at a distance r from their source:

$$G(R, t) = R \left(H + \frac{U^2}{2} \right) \quad (18)$$

In the considered approximation $u^2/c^2 \ll 1$, whereas:

$$R \left(1 - \frac{2U}{c_0} \right) \frac{d^2 R}{dt^2} + \frac{3}{2} \left(1 - \frac{4U}{3c_0} \right) \left(\frac{dR}{dt} \right)^2 + \frac{1}{\rho_0} \left[P_\infty - P(R) \right] + \frac{R U}{\rho_0 c_0} \left(1 - \frac{U}{c_0} \right) \frac{dP(R)}{dR} = 0 \quad (14)$$

where U – the speed of movement of the cavity surface during collapse and pulsation; c_0 – speed of sound in the liquid unaffected by fluctuations.

Flynn supplemented this equation with a term that takes into account the viscosity of the liquid and pressure fluctuations by a harmonic law. As a result, he obtained the following equation:

After necessary transformations, equation (18) looks like this:

$$G = rc \left[U \cdot \left(\frac{R}{r} \right)^2 \right] \cdot \left\{ 1 + \frac{n+1}{4c} \left[U \cdot \left(\frac{R}{r} \right)^2 \right] \right\} \quad (19)$$

where the speed of the cavity surface U is determined by the following transcendental equation:

$$U^2 = \frac{2}{3} \frac{P_0 + P_m}{\rho_0} \left[\frac{R_m^3}{R^3} \left(1 - \frac{U}{3c_0} \right)^4 - 1 \right] \quad (20)$$

The pressure along the shock front can be calculated using the formula given in [16]:

$$p = A \left[\frac{2}{n+1} + \frac{n-1}{n+1} \left(1 + \frac{n+1}{rc_0^2} G \right)^{1/2} \right] \frac{2n}{n-1} - B \quad (21)$$

where B – constant for water ($3.0 \times 10^5 \text{ MPa}$); constants A and n (see Eq. (17)).

Formula (20) makes it possible to analyze the conditions of cavitation effect on the surface of oscillatory system, which creates ultrasonic waves in liquid.

Theory and practice of erosion studies for solid materials in cavitation field.

Erosion of material surfaces in cavitation field occurs following the destruction of bonds in the crystal lattice of the object. Cavitation erosion is determined by the decrease in the mass of the object in the cavitation field, or the state of the photosensitive layer on the glass plate surface. Another variant is to measure the total area of the holes formed in the aluminum foil under the effect of cavitation in a certain period of time. To assess the energy efficiency, Rosenberg introduced the concept of erosion-acoustic efficiency:

$$\eta_{er} = E_m \cdot E \quad (22)$$

where E_m – energy spent on mechanical erosion; E – ultrasonic vibration energy.

The local rate of cavitation-induced destruction in

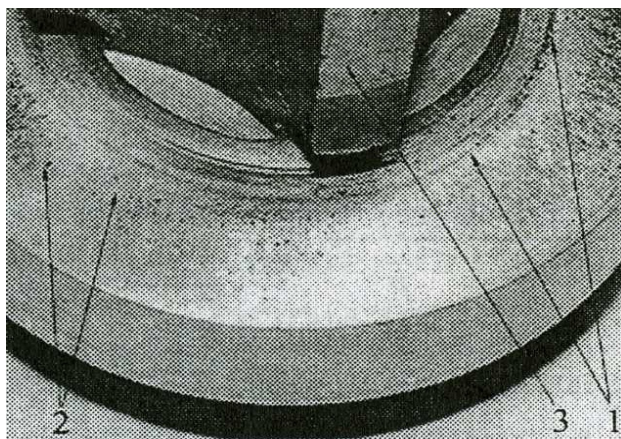


Figure 1 Valve seat of milk homogenizer subjected to cavitation: 1 – erosion canals; 2 – areas of erosion damage to the valve working surface; 3 – guide ways

an inhomogeneous ultrasonic field is determined by the following formula:

$$w_m = \frac{\partial^2 \Delta G}{\partial V dt} \quad (23)$$

where w_m – local rate of erosion in the cavitation field; ΔG – mass of solid particles dispersed in the liquid during erosion that can be separated during analysis; V – the volume of the product (liquid); t – time.

A rather original mathematical apparatus was used to analyze the erosion efficiency of the cavitation field in [6]. Unfortunately, the lack of data makes it impossible to use it for these calculations.

STUDY OBJECTS AND METHODS

This research continues the studies of erosion patterns of cavitation in aquatic environment started at K.G. Razumovsky Moscow State University of Technology and Management [7].

Ultrasound is a promising method of mechanical processing of food masses to produce fine-dispersed systems. However, the product unavoidably comes in contact with the surface of the ultrasonic concentrator, which might result in the diffusion of the solid matter into the liquid medium [8, 9]. This phenomenon is multiplied by vibration, including ultrasound. Figure 1 illustrates erosion on the surface of concentrator (or any other ultrasonic device).

An analytical review of theoretical and experimental studies of cavitation and erosion of solid surfaces in ultrasonic field proved that this process still remains understudied, especially the effect of cavitation on ultrasonic emitters. The theoretical and experimental studies given below represent an initial stage in the research and practical application of data on the interaction between ultrasonic field and ultrasonic emitters, as well as the role of this process in the food safety.

Cavitation produces cavities. When they collapse, they produce an energetic effect on liquid and elements

submerged in it. Ertugay and Sengul described an assessment method for the energy impact of cavitation. Evaluation is carried out on a screen of aluminum or tin foil [8]. When the cavity collapses and as it hits the surface of the foil, dents or tears appear on the screen. The erosive capacity of cavitation is defined by the relative size of the area of dents and tears [14].

The generation of harmonic acoustic vibrations by a solid ultrasonic emitter is a convenient and easily controllable method for producing cavities in liquid medium. Wave theory is the basis for the design of solid emitters. It determines the most active areas of emitters of various shapes. However, it cannot describe the cavitation interactions of individual cavities or their groups [15]. Therefore, the cavitation interactions in ultrasonic fields of various intensities, the propagation of ultrasonic waves, and their ability to create cavities are important research and practical tasks in ultrasonic processing of liquid food media for homogenization, suspensions, and emulsions.

The present research featured cavitation in ultrasonic field created by the cylindrical surface of a solid emitter immersed in distilled water to a depth h . An aluminum foil screen was installed at distance x . The number of cavities was calculated at distance h_1 from the liquid surface in the normal vector to this surface.

Laboratory device IL-10-6/2 was used to create ultrasonic waves as described in [16, 17]. Cavities created by the laboratory installation in the liquid deformed the aluminum foil screen, causing either indentations in the foil or tears in the screen. This kind of violation of the integrity of the screen will be called “holes”.

RESULTS AND DISCUSSION

The technological effect results from ultrasonic cavitation in liquid media as high-density energy localizes in microvolumes of the treated medium.

After a certain amount of pulsations, cavities collapse and trigger a shock wave, which destroys the nearby solid surfaces. Almost all related studies were focused on the process of cavitation-induced destruction of the medium components as a way to increase its homogeneity [18, 19]. The obtained data on kinetics and thermodynamics of cavity formation, time and forms of their existence, etc. make it possible to describe the kinetic and thermodynamic parameters of both cavities and the medium. The part of the ultrasonic device that comes in contact with the processed product is called the “oscillatory system”. The surfaces of oscillatory systems of ultrasonic devices are also subject to cavitation-induced erosion. As a result, a certain amount of the material can mix with the product [20–22].

The present research featured the types and nature of erosion of ultrasonic devices and the safety of the product.

A set of experiments provided foil screens deformed by ultrasonic field. The state of the screen revealed the erosion capabilities of the ultrasonic field generated by



Figure 2 Foil screen deformed by ultrasonic treatment. Processing time – 20 s, distance from the surface of the emitter – 30 mm



Figure 3 Foil screen deformed by ultrasonic treatment. Processing time – 20 s, distance from the surface of the emitter – 150 mm

Table 1 Distribution of deformations on the screen depending on the distance from the surface of emitter x and the distance from the surface of liquid h_1 .

x , mm	h_1 , mm	Distribution of screen deformations at ultrasonic treatment time t and distance h_1			
		5 s	10 s	15 s	20 s
30	5	23	129	115	110
	20	50	126	184	172
	40	104	135	202	304
	60	114	110	125	222
	80	32	31	78	40
		Σ 323	Σ 531	Σ 704	Σ 848
45	5	12	76	140	81
	20	52	196	230	74
	40	51	62	126	60
	60	49	124	112	52
	80	17	40	60	40
		Σ 181	Σ 498	Σ 668	Σ 308
60	5	1	34	24	24
	20	24	58	48	56
	40	116	46	44	44
	60	26	44	42	31
	80	35	31	11	110
		Σ 202	Σ 213	Σ 169	Σ 265
75	5	22	29	40	72
	20	49	61	48	86
	40	37	55	36	32
	60	24	55	155	40
	80	12	54	36	24
		Σ 144	Σ 254	Σ 315	Σ 254
150	5	2	27	10	8
	20	30	26	47	17
	40	40	21	41	30
	60	21	33	27	44
	80	10	14	26	41
		Σ 103	Σ 121	Σ 151	Σ 140
250	5	34	8	15	16
	20	32	24	11	16
	40	26	38	30	25
	60	25	24	34	26
	80	4	4	8	11
		Σ 121	Σ 98	Σ 98	Σ 94
320	5	5	16	25	1
	20	21	10	32	8
	40	38	37	50	20
	60	38	20	24	16
	80	2	9	4	6
		Σ 104	Σ 102	Σ 135	Σ 51

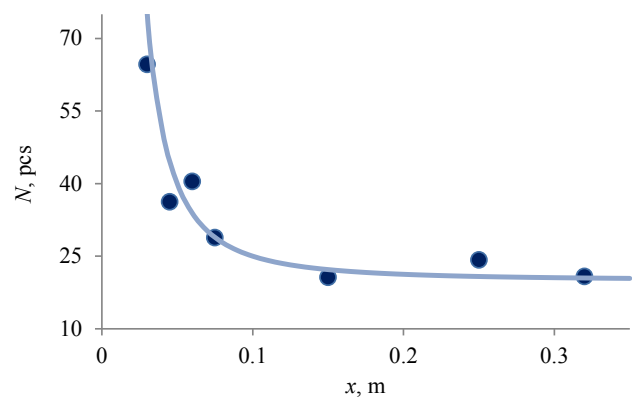


Figure 4 Effect of the distance from the surface of the cylindrical emitter on the amount of screen per 1 s of ultrasonic exposure

a cylindrical acoustic emitter in water. The surface of the screen was also given a cylindrical shape before it was installed in the test medium. The screen was placed in the test medium equidistantly to the surface of the emitter. The exposure of the screen and the curvature of its surface varied in different experiments. Figures 2 and 3 show the aluminum foil screens deformed by ultrasonic treatment.

The surface of the screens indicated a significant inhomogeneity of deformation. However, the agglomeration pattern of acoustic caverns was quite stable in certain areas of the screen surface. The experiments also determined the average value of the density of screen deformations depending on the time of the acoustic impact and the distance from the surface of the emitter (Table 1).

The amount of deformations on the screen decreased as the distance from the surface of the emitter increased.

Figure 4 shows the number of deformations per second (N , pcs) per 0.0004 m^2 of the screen surface, depending on the distance from the surface of the emitter (x , m). The diameter of the emitter was 0.03 m , the depth of immersion was 0.12 m , and the thickness of water layer was 0.25 m .

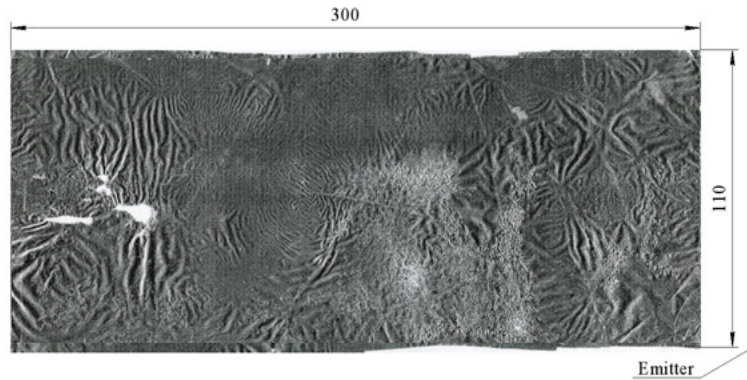


Figure 5 Distribution of cavitation-induced deformations and holes on the screen located equidistantly at distance x from the surface of the cylindrical emitter

Figure 4 illustrates that as the distance from the emitter increased, the amount of screen deformations decreased according to the hyperbolic function:

$$N = a \cdot x^b + c \quad (24)$$

where a , b , and c are constant: $a = 0.05$, $b = 2$, and $c = 20$.

Figure 6 clearly shows the distribution of cavitation-induced deformations after different acoustic exposure periods.

The difference in the distributions shown in Figures 6 and 8 can be explained by such factors as acoustic wind, Bjerknes force, and Stokes force.

Figure 6 suggests that the holes on the radially arranged screen appear as a result of ultrasound waves in the vessel. Thus, the expression for the wave interference for the number of holes will be the following:

$$N = \psi \left[\frac{\sin \left[\left(\frac{2\pi}{T} \right) \left(\frac{x}{c} - t \right) \right]}{\frac{2\pi}{T} \cdot \left(\frac{x}{c} - t \right)} \right]^2 \quad (25)$$

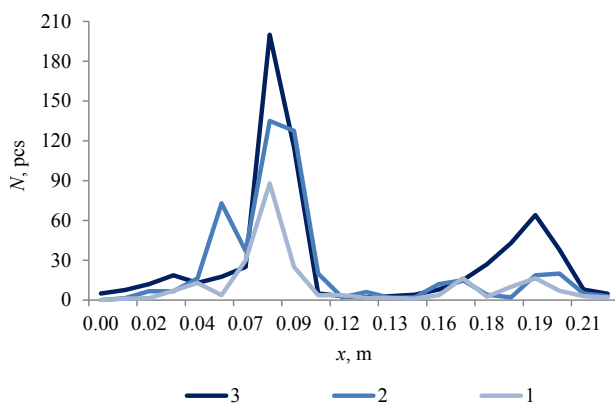


Figure 6 Effect of the distance from the surface of the cylindrical emitter on the distribution of deformations of the radially located screen during 10 s (1), 15 s (2), and 20 s (3)

where ψ – constant equal to the maximum number of cavities on 0.0004 m^2 .

Curves 1 and 2 in Fig. 6 can also be simulated, like curve 3. However, in their cases, the speed of sound is somewhat less than it is universally accepted, i.e. instead of $c = 1500 \text{ m/s}$, it is $c = 1140 \text{ m/s}$ because the water flow is intense and contains air bubbles, which obviously reduces the speed of sound in the water.

The number of holes in the foil screen makes it possible to characterize the energy of cavities formed in this volume. In a first approximation, the work of cavities can be calculated by the following formula:

$$A_E = \frac{4}{3} \pi R_{max}^3 P N \quad (26)$$

where A_E – work produced by the collapsing cavities, W·s; R_{max} – maximal size the cavity reaches as it oscillates around the equilibrium state (max $100 \mu\text{m}$); P – pressure in the cavity as it collapses (10^3 MPa); N – number of cavities per volume.

As the cavity collapses, it produces spherical shock waves (Fig. 8) at a pressure of thousands of MPa. This pressure is much higher than the tensile strength of aluminum, which begins to flow like an ideally plastic body according to Saint-Venant. Therefore, the theory of plasticity can be applied to the theoretical analysis of the effect of shock wave on aluminum foil.

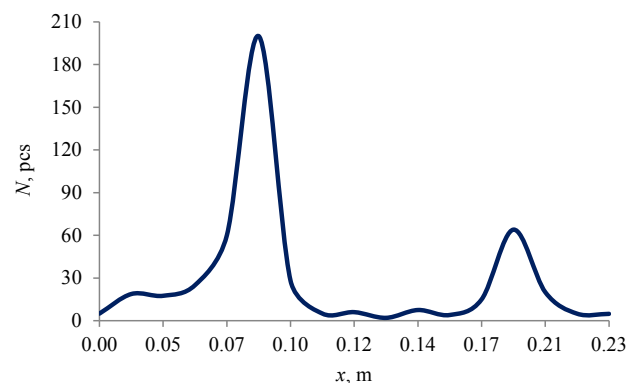


Figure 7 Graphic approximation of curve 3 in Fig. 6

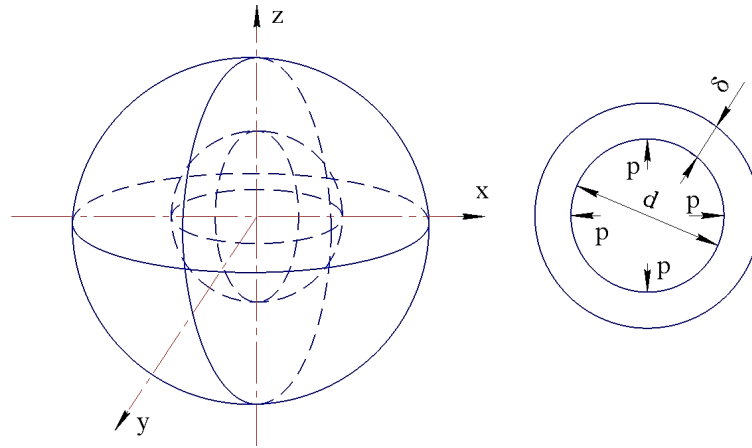


Figure 8 Expansion of hollow sphere made of ideally plastic material under internal pressure

Considering that the area of the foil around the hole formed by the cavity assumes hemispherical shape and that aluminum outside the strength limits behaves like an ideally plastic body, the model of the hole can be represented as the destruction of an ideally plastic sphere by a spherical shock wave (Fig. 9).

The following equation is valid for an ideally plastic body:

$$2(\sigma_r - \sigma_t) + r \frac{d\sigma_r}{dr} = 0 \quad (27)$$

where σ_r and σ_t – normal stresses (tangential and along coordinate r), Pa.

Based on the deformation of the sphere:

$$\sigma_t - \sigma_r = \sigma_f \quad (28)$$

where σ_f – yield stress, Pa.

Considering (27) and (28):

$$d\sigma_r = \pm 2\sigma_f \frac{dr}{r} \quad (29)$$

at $r = d/2$, $\sigma_r = -p_d$; at $r = (d/2) + \delta$, $\sigma_r = -p_g$ where p_g is the hydrostatic pressure of the liquid, Pa.

By integrating (29) under the indicated boundary conditions, we obtain:

$$-p_d = \pm 2\sigma_f \ln(d/2) + C \quad (30)$$

$$-p_g = \pm 2\sigma_f \ln[(d/2) + \delta] + C \quad (31)$$

where C – arbitrary constant.

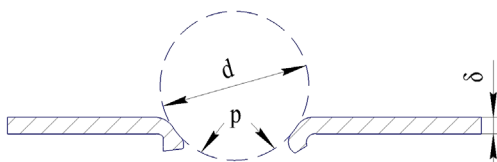


Figure 9 Formation of a hole in the foil under the effect of spherical shock wave as the cavity collapses

Expressing the total pressure of the internal and external hydrostatic (plastic) flow, we get the following equation:

$$p_f = p_d - p_g = \pm 2\sigma_f \ln \frac{[(d/2) + \delta]}{d/2} \quad (32)$$

At $p_d \gg p_g$:

$$p_f = 2\sigma_f \ln \frac{[(d/2) + \delta]}{d/2} \quad (33)$$

The resulting formula (33) makes it possible to calculate the pressure inside the sphere formed by the shock wave after the cavity collapses at a distance close enough to the foil for a hole to occur.

The formula was tested using the data on the ultimate strength of aluminum. The ultimate strength, or the yield condition, of aluminum is $\sigma_f = 60\text{--}100$ MPa.

The size of the holes in the foil varied from 5×10^{-4} to 10^{-6} m. Therefore, the range of pressures in the corresponding cavities can be defined by formula (33).

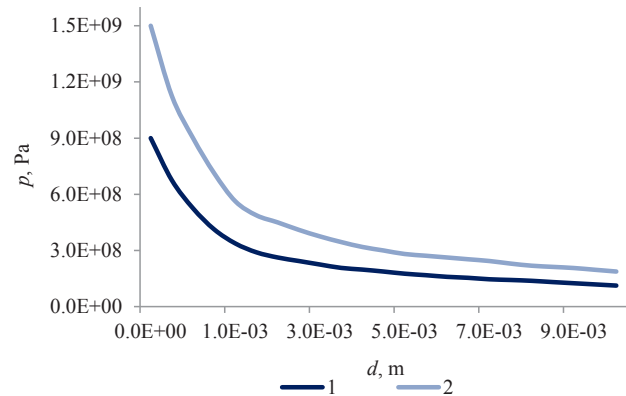


Figure 10 Effect of the diameter of the collapsing cavity on the pressure in spherical shock wave at the strength limits of aluminum = 60 MPa (curve 1) and 100 MPa (curve 2)

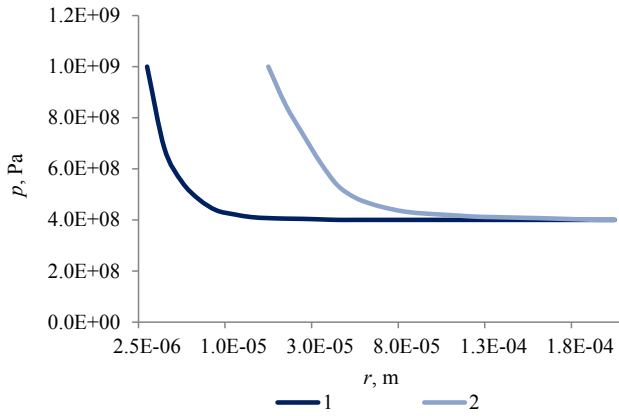


Figure 11 Pressure in the shock wave as calculated by Kirkwood-Bethe formula for distances from the center of the cavity r : the radii of the collapsed cavities – 10^{-5} m (curve 1) and 10^{-6} m (curve 2)

Figure 10 shows the dependences of the pressure in spherical shock wave on the diameter of the collapsing cavity at different strength limits of aluminum.

The pressure in the wave calculated by formula (33) was compared to that calculated by Kirkwood-Bethe formula (17). Figure 11 shows the pressure graph in the shock wave calculated by Kirkwood-Bethe formula for the distances from the center of the cavity r under the collapse of the cavities.

Figures 10 and 11 show that the calculations correlate almost entirely. Therefore, the approach to calculating the collapse pressure in collapsing cavities based on comparing this pressure with the strength of solid materials under erosion can be used to assess the intensity of erosion.

CONCLUSION

The present research revealed the following erosive effect of cavitation on highly rigid materials of ultrasonic vibrating systems.

Figure 12 shows how the corresponding problem from the theory of elasticity can be applied to the task in hand. The spherical shock wave from the collapse of the ultrasonic cavity was considered here as an absolutely rigid ball penetrating into the elastic surface of the ultrasonic emitter.

The problem has the following solution:

$$a = \sqrt[3]{\frac{3\pi kP}{8\beta}} \quad (34)$$

$$q_0 = \sqrt[3]{\frac{24}{\pi^5} \left(\frac{\beta}{k}\right)^2 P} \quad (35)$$

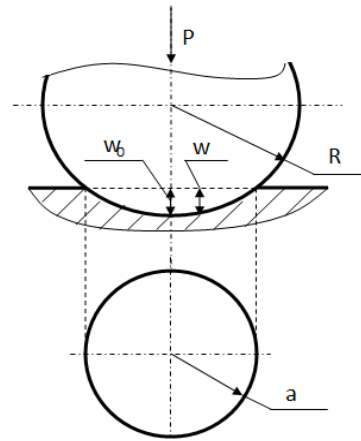


Figure 12 Penetration of an absolutely rigid ball into elastic half-space

$$w_0 = \sqrt[3]{\frac{9\pi^2}{8}\beta k^2 P^2} \quad (36)$$

where a – radius of the contact spot of the ball with radius R with elastic half-space; q and q_0 – current and maximal (in the center of the spot) contact stresses, respectively; $\beta = 1/2R$; $k = (1-\mu^2)/\pi E$; w , w_0 – current and maximal values of the deflection of the elastic space; P – force pushing the ball into the elastic half-space.

The previous studies defined the range of pressure values in cavities. Using these values, assuming that the maximal pressure in the cavity that erodes the emitter, is $p = q_0$, and expressing the size of the contact spot as a and the penetration depth as w_0 via q_0 , we get the following equation:

$$a = q_0 \frac{\pi R(1-\mu^2)}{2E} \quad (37)$$

$$w_0 = \frac{a^2}{R} = R \left[\frac{q_0 \pi (1-\mu^2)}{2E} \right]^2 \quad (38)$$

The obtained results proved that contact spot size a and penetration depth w_0 can serve as a criterion for the erosion of the surface of the ultrasonic emitter.

CONTRIBUTION

The authors were equally involved in the research and are equally responsible for any potential plagiarism or other unethical issues.

CONFLICT OF INTEREST

The authors declare that there are no conflicts of interests regarding the publication on this article.

REFERENCES

1. Chemat F, Rombaut N, Sicaire A-G, Meullemiestre A, Fabiano-Tixier A-S, Abert-Vian M. Ultrasound assisted extraction of food and natural products. Mechanisms, techniques, combinations, protocols and applications: A review. *Ultrasonics Sonochemistry*. 2016;34:540–560. <https://doi.org/10.1016/j.ultsonch.2016.06.035>.
2. Soria AC, Villamiel M. Effect of ultrasound on the technological properties and bioactivity of food: a review. *Trends in Food Science and Technology*. 2010;21(7):323–331. <https://doi.org/10.1016/j.tifs.2010.04.003>.
3. Jadhav AJ, Holkar CR, Goswami AD, Pandit AB, Pinjari DV. Acoustic cavitation as a novel approach for extraction of oil from waste date seeds. *ACS Sustainable Chemistry and Engineering*. 2016;4(8):4256–4263. <https://doi.org/10.1021/acssuschemeng.6b00753>.
4. Ansari JA, Ismail M, Farida M. Investigation of the use of ultrasonication followed by heat for spore inactivation. *Food and Bioprocess Technology*. 2017;104:32–39. <https://doi.org/10.1016/j.fbp.2017.04.005>.
5. Wu H, Hulbert GJ, Mount JR. Effects of ultrasound on milk homogenization and fermentation with yogurt starter. *Innovative Food Science and Emerging Technologies*. 2000;1(3):211–218. [https://doi.org/10.1016/S1466-8564\(00\)00020-5](https://doi.org/10.1016/S1466-8564(00)00020-5).
6. Senrayan J, Venkatachalam S. Ultrasonic acoustic-cavitation as a novel and emerging energy efficient technique for oil extraction from kapok seeds. *Innovative Food Science and Emerging Technologies*. 2020;62. <https://doi.org/10.1016/j.ifset.2020.102347>.
7. Berezovsky YuM, Shpakov VYu, Andreev VN. Experimental assessment of erosive regularities activity cavitation in water. *Tekhnologii 21 veka v pishchevoy, pererabatyvayushchey i legkoy promyshlennosti [Technologies of the XXI century in food, processing, and consumer goods industries]*. 2012;(6–1). (In Russ.).
8. Ertugay MF, Sengul M. Effect of ultrasound treatment on milk homogenisation and particle size distribution of fat. *Turkish Journal of Veterinary and Animal Sciences*. 2004;28(2):303–308.
9. Berezovskii YuM, Dergachev PP, Bliadze VG. Possibilities of milk ultrasonic treatment. *Dairy Industry*. 2009;(5): 46–47. (In Russ.).
10. Ovsyannikov VYu, Toroptsev VV, Berestovoy AA, Lobacheva NN, Lobacheva MA, Martekha AN. Development and research of new method for juice extracting from sugar beet with preliminary pressing. *IOP Conference Series: Earth and Environmental Science*. 2021;640(5). <https://doi.org/10.1088/1755-1315/640/5/052011>.
11. Vasiliev AM, Bredihin SA, Andreev VK. To the question of non-harmonic force oscillations and moment by the vibration generator. *IOP Conference Series: Earth and Environmental Science*. 2021;640(7). <https://doi.org/10.1088/1755-1315/640/7/072011>.
12. Wang T, Guo N, Wang S-X, Kou P, Zhao C-J, Fu Yu-J. Ultrasound-negative pressure cavitation extraction of phenolic compounds from blueberry leaves and evaluation of its DPPH radical scavenging activity. *Food and Bioprocess Technology*. 2018;108:69–80. <https://doi.org/10.1016/j.fbp.2018.01.003>.
13. Huang L, Zhang W, Ding X, Wu Z, Li Y. Effects of dual-frequency ultrasound with different energy irradiation modes on the structural and emulsifying properties of soy protein isolate. *Food and Bioprocess Technology*. 2020;123: 419–426. <https://doi.org/10.1016/j.fbp.2020.07.021>.
14. Chakraborty S, Uppaluri R, Das C. Optimization of ultrasound-assisted extraction (UAE) process for the recovery of bioactive compounds from bitter melon using response surface methodology (RSM). *Food and Bioprocess Technology*. 2020;120:114–122. <https://doi.org/10.1016/j.fbp.2020.01.003>.
15. Zhang L, Zhou C, Wang B, Yagoub AE-GA, Ma H, Zhang X, et al. Study of ultrasonic cavitation during extraction of the peanut oil at varying frequencies. *Ultrasonics Sonochemistry*. 2017;37:106–113. <https://doi.org/10.1016/j.ultsonch.2016.12.034>.
16. Scudino H, Silva EK, Gomes A, Guimaraes JT, Cunha RL, Sant'Ana AS, et al. Ultrasound stabilization of raw milk: Microbial and enzymatic inactivation, physicochemical properties and kinetic stability. *Ultrasonics Sonochemistry*. 2020;67. <https://doi.org/10.1016/j.ultsonch.2020.105185>.
17. Potoroko I, Kalinina I, Botvinnikova V, Krasulya O, Fatkullin R, Bagale U, et al. Ultrasound effects based on simulation of milk processing properties. *Ultrasonics Sonochemistry*. 2018;48:463–472. <https://doi.org/10.1016/j.ultsonch.2018.06.019>.
18. Silva M, Zisu B, Chandrapala J. Influence of low-frequency ultrasound on the physico-chemical and structural characteristics of milk systems with varying casein to whey protein ratios. *Ultrasonics Sonochemistry*. 2018;49: 268–276. <https://doi.org/10.1016/j.ultsonch.2018.08.015>.
19. Patil L, Gogate PR. Ultrasound assisted synthesis of stable oil in milk emulsion: Study of operating parameters and scale-up aspects. *Ultrasonics Sonochemistry*. 2018;40:135–146. <https://doi.org/10.1016/j.ultsonch.2017.07.001>.

20. Ovsyannikov VYu, Berestovoy AA, Lobacheva NN, Toroptsev VV, Trunov SA. Research of the process of vegetable oil extracting under the influence of a high frequency wave field. IOP Conference Series: Materials Science and Engineering. 2020;941(1). <https://doi.org/10.1088/1757-899X/941/1/012052>.
21. Krasulya O, Bogush V, Trishina V, Potoroko I, Khmelev S, Sivashanmugam P, et al. Impact of acoustic cavitation on food emulsions. Ultrasonics Sonochemistry. 2016;30:98–102. <https://doi.org/10.1016/j.ultsonch.2015.11.013>.
22. Shalunov AV, Khmelev VN, Terentiev SA, Nesterov VA, Golykh RN. Ultrasonic dehydration of food products with moisture removal without phase transition. Food Processing: Techniques and Technology. 2021;51(2):363–373. (In Russ.). <https://doi.org/10.21603/2074-9414-2021-2-363-373>.

ORCID IDs

Sergei A. Bredihin  <https://orcid.org/0000-0002-6898-0389>
Vladimir N. Andreev  <https://orcid.org/0000-0002-4890-379X>
Alexander N. Martekha  <https://orcid.org/0000-0002-7380-0477>
Matthias G. Schenzle  <https://orcid.org/0000-0001-6334-0481>
Igor A. Korotkiy  <https://orcid.org/0000-0003-4379-9652>